INL/CON-23-73263-Revision-1

CNRS Molten Salt Reactor Benchmark Analysis Using Griffin-Pronghorn Coupled Multi-physics Code System

November 2023

Namjae Choi, Mustafa Kamel Mohammad Jaradat

Changing the World's Energy Future

Idaho National Laboratory

INL is a U.S. Department of Energy National Laboratory operated by Battelle Energy Alliance, LLC

INL/CON-23-73263-Revision-1

CNRS Molten Salt Reactor Benchmark Analysis Using Griffin-Pronghorn Coupled Multi-physics Code System

Namjae Choi, Mustafa Kamel Mohammad Jaradat

November 2023

Idaho National Laboratory
Idaho Falls, Idaho 83415

http://www.inl.gov

Prepared for the
U.S. Department of Energy
Under DOE Idaho Operations Office
Contract DE-AC07-05ID14517

CNRS Molten Salt Reactor Benchmark Analysis Using Griffin-Pronghorn Coupled Multi-physics Code System

Namjae Choi, Mustafa Jaradat

Idaho National Laboratory, 1955 Fremont Ave., Idaho Falls, ID 83415
Namjae.Choi@inl.gov, Mustafa.Jaradat@inl.gov

INTRODUCTION

Molten salt reactors (MSRs) with flowing fuel have the unique feature of utilizing the fuel salt for heat generation and extraction at the same time, since the fuel salt is circulating through the whole primary loop. This movement of fuel salt results in a partial decay of the delayed neutron precursors (DNPs) outside the core and the corresponding redistribution of the DNPs in the active region of the core. To capture this effect, neutronics and thermal-hydraulics (T/H) codes need to be able to handle the movement of DNPs and their decay [1, 2].

Idaho National Laboratory (INL) is actively working on developing the neutronics and T/H codes to model the MSRs with flowing fuel. As one of the efforts, the neutronics code Griffin [3] and the T/H code Pronghorn [4] that are built upon the MOOSE framework [5] have been extended to handle the flowing fuel involving the drift of DNPs, and this capability is being tested and verified with MSR benchmark problems including the CNRS benchmark problem [6]. Additionally, a multi-physics analysis of the molten salt reactor experiment (MSRE) is being conducted to verify and validate the codes against available experimental data [7].

This work presents the analysis of the CNRS benchmark problem using the Griffin-Pronghorn coupled multi-physics code system of INL. Both steady-state and transient problems are analyzed, and the results are compared with those of other participants presented in [6]. The following section provides a description of the benchmark, along with input parameters and observables for each step. Then, the results for each step are presented in comparison with other participants' results, followed by summary and conclusion.

BENCHMARK DESCRIPTION

The geometry of the CNRS benchmark is shown in Fig. 1. It represents a simple 2D lid-driven cavity of a 2 m × 2 m domain filled with fluoride salt with U-235 as the fissile. The cross section data and the T/H properties of the problem can be found in [6]. Only the fuel salt density change by thermal expansion was considered as the main temperature feedback mechanism and the Doppler broadening of cross sections is not taken into account.

The benchmark analysis is performed in three phases: (1) single-physics (stand-alone neutronics or T/H) steady-state tests (phase 0), (2) multi-physics coupled steady-state tests (phase 1), and (3) multi-physics coupled transient tests (phase 2). The input parameters and the output observables of each benchmark step are summarized in TABLE I and TABLE II.

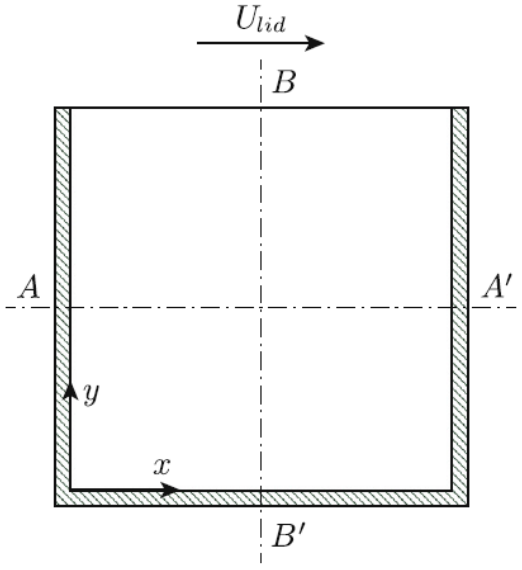

Fig. 1. CNRS benchmark problem geometry [6].

TABLE I. Benchmark input parameters of each step.

0.1	- U_{lid} = 0.5 m/s
0.2	- T = 900 K - P = 1.0 GW
0.3	- Fixed flow field from Step 0.1 - Fixed heat source distribution from Step 0.2 - $\gamma = 1 \times 10^{-6}$ W/m^{3}K
1.1	- Fixed flow field from Step 0.1 - T = 900 K - P = 1.0 GW
1.2	- Fixed flow field from Step 0.1 - P = 1.0 GW - $\gamma = 1 \times 10^{-6}$ W/m^{3}K
1.3	- P = 1.0 GW - U_{lid} = 0.0 m/s - $\gamma = 1 \times 10^{-6}$ W/m^{3}K
1.4	- $\gamma = 1 \times 10^{-6}$ W/m^{3}K - P variable in the range [0, 1] GW, with a step of 0.2 - U_{lid} variable in the range [0, 0.5] m/s, with a step of 0.1
2.1	- Steady-state solution from Step 1.4 with U_{lid} = 0.5 m/s and P = 1.0 GW - $\gamma = 1 \times 10^{-6}$ W/m^{3}K

TABLE II. Benchmark observables of each step.

0.1	- Velocity components along centerlines AA′ and BB′
0.2	- Fission rate density along AA′ - Reactivity ρ
0.3	- Temperature distribution along centerlines AA′ and BB′
1.1	- Delayed neutron source along AA′ and BB′ - Reactivity change from Step 0.2, ρ - $\rho_{0.2}$
1.2	- Temperature distribution along AA′ and BB′ - Reactivity change from Step 1.1, ρ - $\rho_{1.1}$ - Change of fission rate density along AA′ and BB′ with respect to the solution obtained at Step 0.2
1.3	- Velocity components and temperature distribution along AA′ and BB′ - Delayed neutron source along AA′ and BB′ - Reactivity change from Step 0.2, ρ - $\rho_{0.2}$
1.4	- Reactivity change from Step 0.2, ρ - $\rho_{0.2}$, as a function of P and U_{lid}
2.1	- Power gain and phase shift as a function of the perturbation frequency.

VERIFICATION RESULTS

In this section, the results of each phase and step will be presented in comparison to the other benchmark participants' results with a brief description of the results. The diffusion solver was used in Griffin with 200 × 200 mesh.

Phase 0: Single-physics Benchmark

This phase is designed to verify single-physics steady-state solutions. Step 0.1 compares the steady-state velocity field of the fuel salt for a given fixed lid velocity of 0.5 m/s. The horizontal velocity component along line BB′ calculated by Pronghorn is presented in Fig. 2, which agrees very well with the other results reported in the benchmark.

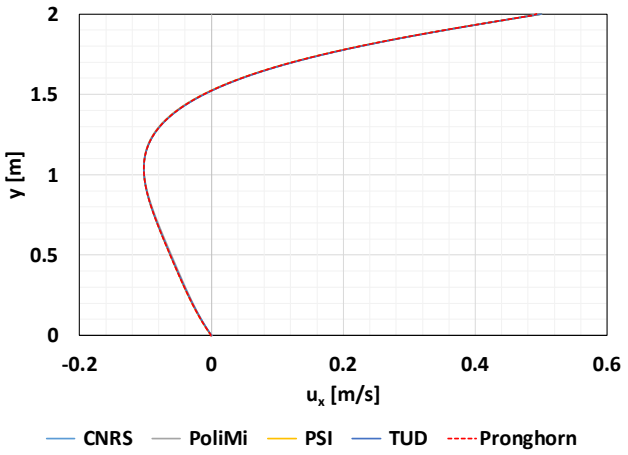

Fig. 2. Step 0.1 – Horizontal velocity component along BB′.

Step 0.2 compares the steady-state neutronics solutions. TABLE III presents the reactivity and Fig. 3 demonstrates the fission rate density along line AA′. The reactivity calculated by Griffin is 465.7 pcm, and it is 22.6 pcm higher than the average of the reported values, but it is reasonable given the large variance of the reported values. In the meantime, the fission rate density agrees very well with the other results.

TABLE III. Step 0.2 – Reactivity.

Code	**ρ [pcm]**
CNRS (SP1 / SP3)	411.3 / 353.7
PoliMi	421.2
PSI	411.7
TUD (S2 / S6)	482.6 / 578.1
Avg.	443.1
Griffin (Diff.)	465.7 (22.6)

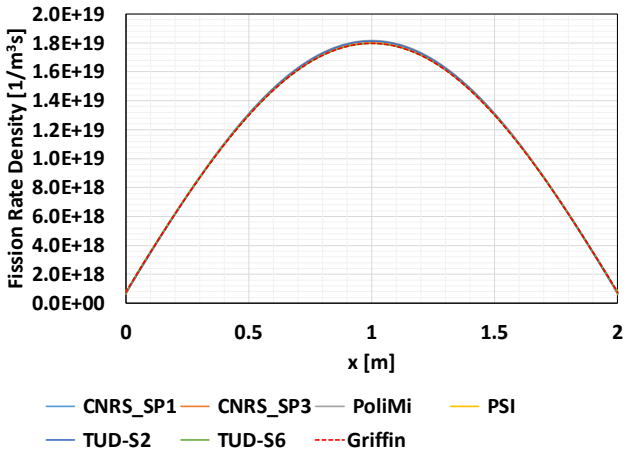

Fig. 3. Step 0.2 – Fission rate density along AA′.

Step 0.3 compares the steady-state temperature profile, with the velocity field of Step 0.1 and the heat source of Step 0.2 as inputs. Fig. 4 shows the temperature profile calculated by Pronghorn along line BB′, and it also agrees very well with the other results, which is already expected given the good agreements in Step 0.1 and 0.2.

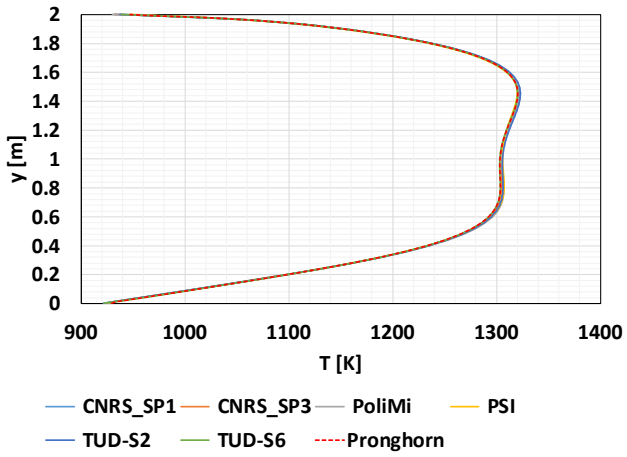

Fig. 4. Step 0.3 – Temperature along BB′.

Phase 1: Steady-State Coupling

This phase compares multi-physics coupled steady-state results. Step 1.1 assesses the impact of DNP drift in the cavity on the reactivity and the delayed neutron source distribution with the fixed velocity field from Step 0.1 and the constant temperature of 900K. TABLE IV shows the reactivity change from Step 0.2, and the Griffin result differs from the average only by 0.7 pcm. And Fig. 5 illustrates the delayed neutron source along line BB′, which is slightly top-skewed by the DNP drift and is consistent with the other results.

TABLE IV. Step 1.1 – Reactivity change from Step 0.2.

Code	$\rho - \rho_{0.2}$ [pcm]
CNRS (SP1 / SP3)	-62.5 / -62.6
PoliMi	-62.0
PSI	-63.0
TUD (S2 / S6)	-62.0 / -60.7
Avg.	-62.1
Griffin (Diff.)	-61.4 (0.7)

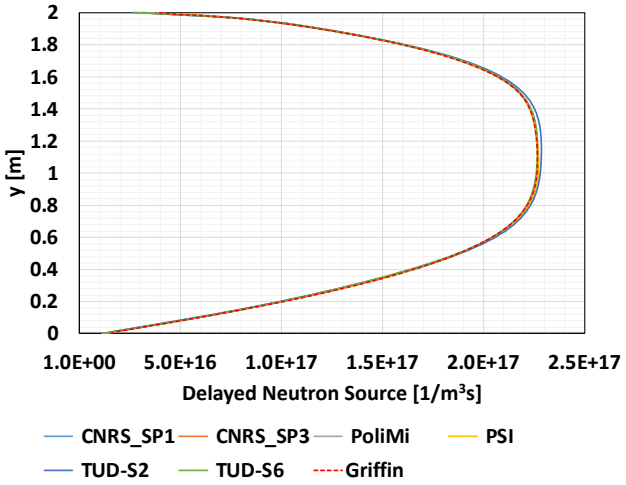

Fig. 5. Step 1.1 – Delayed neutron source along BB′.

Step 1.2 adds in the temperature feedback to Step 1.1 and assesses its impact to the reactivity and fission rate density distribution. TABLE V compares the reactivity change from Step 1.1, and Fig. 6 presents the fission rate density change from Step 0.2 along line AA′. Both the reactivity change and the fission rate density change are in a good agreement with the other results, with the reactivity change differing by only -1.3 pcm from the average.

TABLE V. Step 1.2 – Reactivity change from Step 1.1.

Code	$\rho - \rho_{1.1}$ [pcm]
CNRS (SP1 / SP3)	-1152.0 / -1152.7
PoliMi	-1161.0
PSI	-1154.8
TUD (S2 / S6)	-1145.2 / -1122.0
Avg.	-1148.0
Griffin (Diff.)	-1149.3 (-1.3)

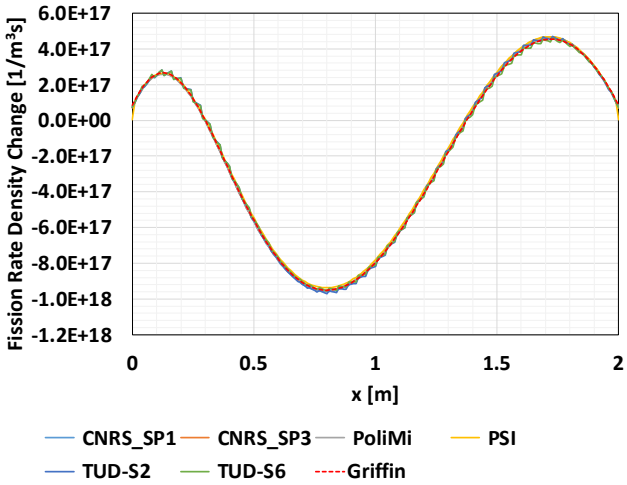

Fig. 6. Step 1.2 – Fission rate density change from Step 0.2 along AA′.

Step 1.3 assesses the ability to perform a fully-coupled simulation including the velocity fields for a system without forced convection, namely the lid velocity being zero, where the flow is only driven by the buoyancy effect caused by the temperature gradient. TABLE VI shows the reactivity change from Step 0.2, and Fig. 7 shows the delayed neutron source distribution along line AA′. The difference in the reactivity change with the average is only 1.5 pcm, and the delayed neutron source also matches closely with the other results.

TABLE VI. Step 1.3 – Reactivity change from Step 0.2.

Code	$\rho - \rho_{0.2}$ [pcm]
CNRS (SP1 / SP3)	-1220.5 / -1220.7
PoliMi	-1227.0
PSI	-1219.6
TUD (S2 / S6)	-1208.5 / -1184.4
Avg.	-1213.5
Griffin (Diff.)	-1212.0 (1.5)

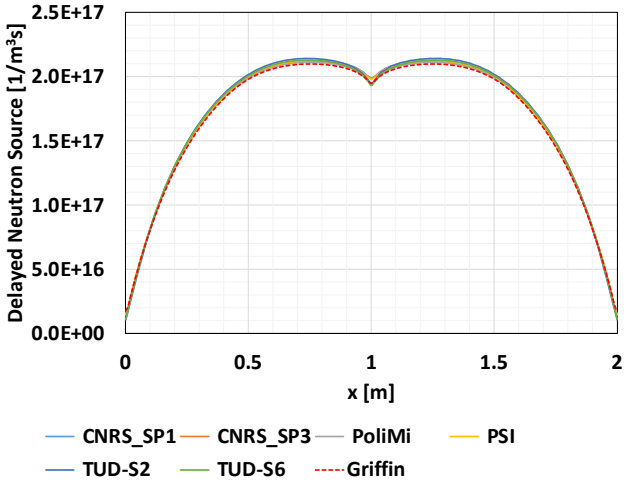

Fig. 7. Step 1.3 – Delayed neutron source along AA′.

Finally, Step 1.4 assesses fully-coupled simulations for various combinations of power level and lid velocity, which is basically the generalization of Step 1.3. TABLE VII shows the reactivity change from Step 0.2 of each combination, and in every case the difference with the average does not exceed ± 2.5 pcm, which proves that the Griffin-Pronghorn coupled code system is sound for a wide range of T/H conditions.

TABLE VII. Step 1.4 – Reactivity change from Step 0.2.

	U_{lid} [m/s]	$\rho - \rho_{0.2}$ [pcm]				
		P [GW]				
		0.2	**0.4**	**0.6**	**0.8**	**1.0**
Avg.	**0.0**	-264.3	-499.3	-732.8	-969.3	-1212.7
Griffin		-263.4	-499.3	-733.3	-970.4	-1212.0
Diff.		0.9	0.0	-0.5	-1.1	0.7
Avg.	**0.1**	-267.1	-499.9	-732.6	-969.2	-1211.6
Griffin		-265.6	-499.6	-733.0	-969.8	-1211.0
Diff.		1.5	0.3	-0.4	-0.6	0.6
Avg.	**0.2**	-269.8	-500.0	-731.3	-966.7	-1208.5
Griffin		-267.7	-499.7	-731.8	-966.8	-1208.0
Diff.		2.1	0.3	-0.5	-0.1	0.5
Avg.	**0.3**	-270.8	-500.1	-730.2	-964.1	-1204.5
Griffin		-269.5	-499.3	-730.0	-963.9	-1203.8
Diff.		1.3	0.8	0.2	0.2	0.7
Avg.	**0.4**	-273.7	-500.1	-729.2	-961.7	-1200.7
Griffin		-271.3	-499.1	-728.5	-961.3	-1200.0
Diff.		2.4	1.0	0.7	0.4	0.7
Avg.	**0.5**	-276.0	-500.9	-728.7	-960.5	-1197.8
Griffin		-273.5	-499.1	-727.5	-959.3	-1196.9
Diff.		2.5	1.8	1.2	1.2	0.9

Phase 2: Transient Coupling

This phase consists of a single step and is dedicated for verifying multi-physics coupled transient calculations. The heat transfer coefficient γ is changed in time by a sinusoidal perturbation with the amplitude of 10% of the original value and with the varying frequencies of 0.0125, 0.025, 0.05, 0.1, 0.2, 0.4, and 0.8 Hz. This leads to a sinusoidal behavior of the reactor power from which the power gain and the phase shift of power from γ can be computed. Fig. 8 and Fig. 9 show the power gain and the phase shift as a function of the frequency, respectively, and at all the frequencies the Griffin results are consistent with the other results.

SUMMARY AND CONCLUSION

In this work, the MSR flowing fuel modeling capabilities of the Griffin-Pronghorn coupled code system of INL were verified employing the CNRS MSR benchmark problem. The benchmark encompasses single- and multi-physics, steady-state and transient problems, and the coupled code system proved its soundness for all the cases. The code system is still under active verification and validation, and its application to more complex and realistic MSR problems will be presented in the future.

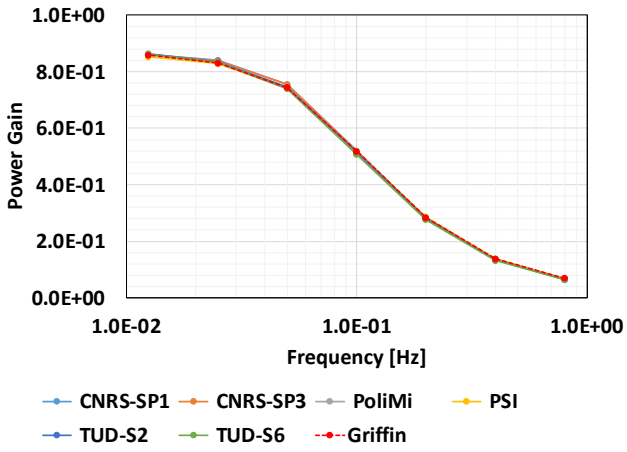

Fig. 8. Step 2.1 – Power gain.

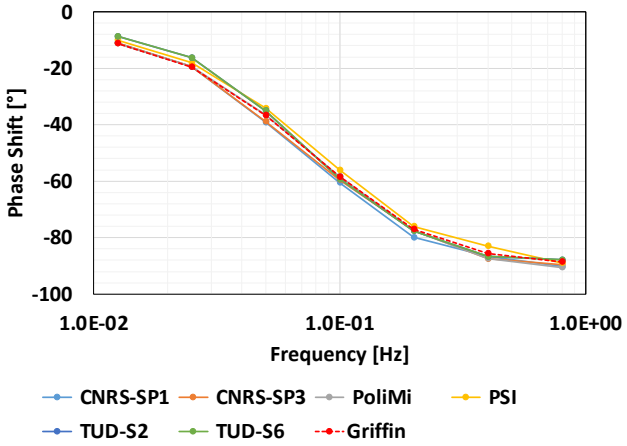

Fig. 9. Step 2.1 – Phase shift.

REFERENCES

1. M. Jaradat *et al.*, "Development and validation of PROTEUS-NODAL transient analyses capabilities for molten salt reactors," *Annals of Nuclear Energy* 160, no. 108402 (2021).
2. G. Yang *et al.*, "Development of coupled PROTEUS-NODAL and SAM code system for multiphysics analysis of molten salt reactors," *Annals of Nuclear Energy* 168, no. 108889 (2022).
3. Y. Wang *et al.*, "Rattlesnake: A MOOSE-Based Multiphysics Multischeme Radiation Transport Application," *Nuclear Technology* 207 (7), pp. 1047–1072 (2021).
4. A. Novak *et al.*, "Pronghorn: A Multidimensional Coarse-Mesh Application for Advanced Reactor Thermal Hydraulics," *Nuclear Technology* 207 (7), pp. 1015–1046 (2021).
5. A. Lindsay *et al.*, "2.0 – MOOSE: Enabling massively parallel multiphysics simulation," *SoftwareX* 20, no. 101202 (2022).
6. M. Tiberga *et al.*, "Results from a multi-physics numerical benchmark for codes dedicated to molten salt fast reactors," *Annals of Nuclear Energy* 142, no. 107428 (2020).
7. M. Jaradat, J. Ortensi, "Thermal spectrum molten salt-fueled reactor reference plant model," Idaho National Laboratory, INL/RPT-23-72875 (2023).